Supercooling suppression and thermal behavior improvement of erythritol as phase change material for thermal energy storage

Yi Wang[a,b,*], Shuang Li[b], Ting Zhang[b], Deyi Zhang[a], Hui Ji[b]

[a] State Key Laboratory of Advanced Processing and Recycling of Nonferrous Metals, Lanzhou University of Technology, Lanzhou 730050, PR China
[b] College of Petrochemical Technology, Lanzhou University of Technology, Lanzhou 730050, PR China

ARTICLE INFO

ABSTRACT

The main aim of this paper is to mitigate the supercooling and improve the heat release performance of erythritol (ET) as phase change material for thermal energy storage using the method of encapsulation and doping additives. The capsules containing ET, thickening and nucleating agent were prepared and various characterization techniques were employed to investigate the structure and thermo-physical properties of the composite, especially the supercooling inhibition and exothermicity improvement. Experimental results reveal that capsulation and adding thickening and nucleating agents have positive influence on the supercooling elimination, heat discharging ability improvement and thermal stability enhancement. The optimal capsules, with the maximal ET mass percentage of 59.2%, melt at 121.2 °C and freeze at 106.4 °C with the latent heat of 213.3 J/g and 206.9 J/g, respectively. Due to the improved crystallization kinetics, the degree of supercooling decreased by 83.6% as well as the heat release ratio increased by 52.2% compared to those of pristine ET. The as-prepared capsules have obvious core-shell structure, good compatibility between the shell and core materials. The thermal conductivity is 0.84 W/m K, increased by 29.2% than that of pristine ET. The results of accelerated thermal cycling test indicate that the supercooling, heat release ability and thermal reliability of encapsulated ET changed imperceptibly. In total, the technology of capsulation and adding thickening and nucleating agents can be used to suppress the supercooling and improve the thermal behavior of ET.

1. Introduction

Latent heat thermal energy storage (LHTES) is one of the most competent ways, and now emerging with considerable momentum for developing renewable energy and improving the efficiency of energy utilization [1]. The thermal energy storage medium in LHTES is called phase change material (PCM) which is characterized by storing or releasing large amount of latent heat while changing from one phase to another within a small range or at a specific temperature [1,2]. Until now, more than 160,000 [3] chemical substances including salt hydrates, polyols, paraffins, fatty acids, fatty acid esters and their mixtures were investigated as PCM to meet a variety of freezing/melting points [4]. From the literature review, the PCMs with the phase change temperature between 0 and 60 °C aiming to low temperature application, e.g. building energy conservation, domestic heating/cooling and biomedical products, received more attention [5,6], while the PCMs with melting point about 100 °C were seldom to survey relatively. In fact, this emerging PCM category is more suitable for recovering industrial high-temperature waste heat, producing domestic hot water and

manufacturing cold water through an absorption chiller [7]. According to a reliable PCMs' database, erythritol (ET) appears to be a more suitable candidate than other less expensive organics like paraffin and fatty acids owing to its moderate phase change temperature [8]. Erythritol [$(CH_2OH)(CHOH)_2(CH_2OH)$, CAS No.149-32-6], a meso-compound of 1,2,3,4-butanetetrol prepared industrially by glucose fermentation using inexpensive raw as carbon sources [9], exhibits excellent thermo-chemical properties such as good thermal stability, high mass-specific enthalpy (about 340 J/g [9,10] −379 J/g [11,12]), considerable specific heat (1.68 $J/g\,K^{-1}$ [13]) and moderate phase change temperature (approx. 118 °C) [12,14]. Besides these, the four-carbon sugar alcohol also has the features of renewable origin being plants-based which determines the attributes of safety (even for daily uptake as a common sweetener) [9], environment friendly [15], cost-effectiveness and high compatibility with container [16]. Even so, the knowledge on the thermo-physical properties and phase change behaviors of ET as a desirable PCM for thermal energy storage design is presently sparse and rather inconsistent [8].

The main reason of the scarce information about the four-carbon

---

* Correspondence to: State Key Laboratory of Advanced Processing and Recycling of Non-ferrous Metals, Lanzhou University of Technology, No. 287, Langongping Road, Lanzhou, Gansu 730050, PR China.
E-mail addresses: wangyi@lut.cn, haoyunwangyi1977@163.com (Y. Wang).

sugar alcohol using as PCM may attribute to its inherent drawback of serious mismatch between heat storage and release performance and severe supercooling more than 100 °C [16]. Although almost all of literatures reported that ET possesses a high fusion heat which is much higher than most of molten salts and waxes, the freezing enthalpy of ET is depressed and often is selectively forgotten. As far as we know, only A. Sari [11,12] clearly indicated that ET melt at 118.4 °C with the latent heat of 379.57 J/g and freeze at 36.22 °C with the enthalpy of 255.95 J/g. This solidification enthalpy is about 32.6% less than fusion enthalpy means that only about 67.4% of stored thermal energy can be used. Obviously, this mismatch makes thermal energy storage deviated from the original pathway and it is not acceptable in practical application because ET will not discharge the stored thermal energy in the subsequent use. Therefore, it seems worthwhile to further evaluate the suitability of ET as a PCM and detailedly understand the thermal energy storage performance. The second flaw of ET is its serious supercooling (super cooling, also called subcooling [17]) which is a state where liquid PCMs do not solidify immediately at the normal melting (or freezing) temperature, but start crystallization only after a temperature well below the melting temperature is reached [17–20]. Due to the effects of supercooling, it is difficult to control the heat recovery at a constant temperature, which in turn leads to the quality and application fields reduce of the released heat.

Poor nucleation characteristic and slow crystal growth rate are widely considered to be the possible causes of supercooling for ET [21,22] although the mechanism of supercooling is still not clearly understood [21]. Different attempts were conducted to prevent supercooling or reduce it to a minimum level such as adding nucleating agent or nanoparticle additives [19,20], controlling of the size of the PCM [14,23,24], employing mechanical energy including mechanical vibration, stirring and ultrasonic irradiation [21,22]. I. Kholmanov [19] demonstrated that the continuous ultrathin graphite foams (UGFs) could strongly reduce the subcooling degree of erythritol, 79 ± 4 K to 67 ± 4 K, due to the heterogeneous nucleation of erythritol at interfaces with the graphitic structures. M. Karthik [25] declared that the subcooling behavior of ET in ET/graphite foam composite was reduced up to 55 °C. Y. Liu [20,26] investigated the effects of graphene oxide nanosheets and ultrasonic oscillation on the supercooling degree and nucleation behavior of nanofluids PCMs experimentally and analytically, and the results showed that the supercooling degree and nucleation time reduced by 69.1% and 90.7%, respectively. E.P. Ona [21,22] revealed that ultrasonic irradiation is beneficial for the supercooling relaxation and solidification enhancement of erythritol because ultrasonic irradiation enabled constant fragmentation and effective dispersion of crystals. T. Adachi [23] revealed that the supercooling duration of ET in a glass tube increased with the decrease of supercooling degree and specimen size. L. L. Wei [27] measured the supercooling degree for ET masses from 10 mg to 20 g and revealed that the supercooling degree monotonic increased with the decrease of specimen mass [23].

Recently, micro- or nano- encapsulation technology was also employed to reduce supercooling degree of PCMs. A. Sari [28] and G. Fang [29] indicated that microencapsulation could slightly decrease the supercooling degree of the PCMs. At the same time, Y. Wang [30], X. Tang [31] and S. N. Gunasekara [8] declared that the supercooling is effectively suppressed when it is nanoencapsulated. However, some of researches also reported the opposite discoveries, which claim that there is significant decrease of crystallization temperature and obvious increase of supercooling degree during the freezing process with the dropping of microcapsules diameter [18,32–34]. As an example, M. You [32] described that the crystallization temperature of styrene-divinybenzene *co*-polymer containing *n*-octadecane (C18) microcapsules was about 10 °C lower than that of pristine PCM. On the other hand, voluminous evidence suggests that dispersing nucleating agent or adding thickening agent prior to encapsulate, such as employing aliphatic alcohol as nucleating agent for short-chain *n*-alkanes [34–36], will

resulted in the reduction of supercooling degree and short of solidification or melting time. However, influences of nucleating agent and thicker on the enthalpy of microencapsulated PCMs (MEPCMs) have not been studied, especially for capsules containing ET.

Preparing microcapsules containing ET for high temperature application, the cornerstone of further investigation about the influence of encapsulation and additive on the crystallization behavior and heat storage/release ability, is still a challenge at present due to the technical difficulties [5,14]. Firstly, as a kind of water-soluble PCM, ET is much more difficult to prepare MEPCMs than oil-soluble PCMs [1,37] since most of fabricating method using water as solvent. Thus, there are rarely studies on MCPCMs with water-soluble PCM. Secondly, ET has an annoying operating temperature (higher than 120 °C). The high phase transition temperature does not only lead to manufactural difficulty, but also increase the risk of crack in the subsequent usage which generated by the different volumetric thermal expansion coefficient of PCM and shell [5,14,38]. Therefore, preparing ET based capsules and further understanding the relationship between the encapsulation, impurities kinds and amounts on the thermal behavior of ET are necessary and challenging works.

In light of the above discussion, the overall objective of this work is to develop a feasible fabrication technique for the form-stable ET MEPCMs, improve the thermal behavior of ET as a potential PCM for low grade thermal energy storage and further understand the effect of encapsulation, impurity addition on the supercooling suppression. Toward these ends, the encapsulation of embedding erythritol into polysiloxane (pSiO) network for the preparation of ET/pSiO composite MEPCMs through ultraviolet assists hydrolysis method has been studied, and the effects of encapsulation conditions, amounts of nucleating and thickening agent on the crystallization behavior, especially on the thermal release properties and subcooling degree of ET were investigated. Also, the morphology, structure, thermal reliability and stability, thermal conductivity, heat storage properties of the composite which prepared in the optimum technical conditions, together with those of ET and/or pSiO for comparison purpose, were determined by Fourier transformation infrared spectroscopy (FT-IR), scanning and transmission electron microscope (SEM and TEM), thermogravimetric analysis (TGA), differential scanning calorimetry (DSC), X-ray diffraction (XRD) and accelerated thermal cycling test (ATC).

2. Experimental

2.1. Materials

Erythritol (ET, commercial grade), used as phase change material without further purification, was purchased from Tianjin Baishi chemical industry Co. Ltd., China. 3-Methacryloxypropyltrimethoxysilane (MEMO, CAS No.2530-85-0) was sourced from Aladdin, Shanghai biological technology Co. Ltd. and employed as precursor of shell material. Carboxymethylcellulose (CMC) and nano-alumina (α-Al$_2$O$_3$) were selected as thickening and nucleating agent, which supplied by Dadi chemical Co. Ltd., Hangzhou China and Shanghai Zhongli Chemical Co., Ltd, respectively. The other chemicals, ethanol, benzene, toluene and sorbitan monooleate (Span-80), were all designated to be of analytical grade and received from Shanghai Chemical Reagent Co. Ltd. Deionized water consumed in all fabricated recipes was self-made by our laboratory.

2.2. Methods

The form-stable blends were synthesized by ultraviolet assisted hydrolysis method aiming to shorten the polycondensation time of MEMO and improve the yield of the products. The mechanism of designed fabrication may be divided into two steps, hydrolysis, directional adsorption and condensation, which is shown in Fig. 1. A typical synthetic process is described as follows: (1) 10 mL saturated solution of ET
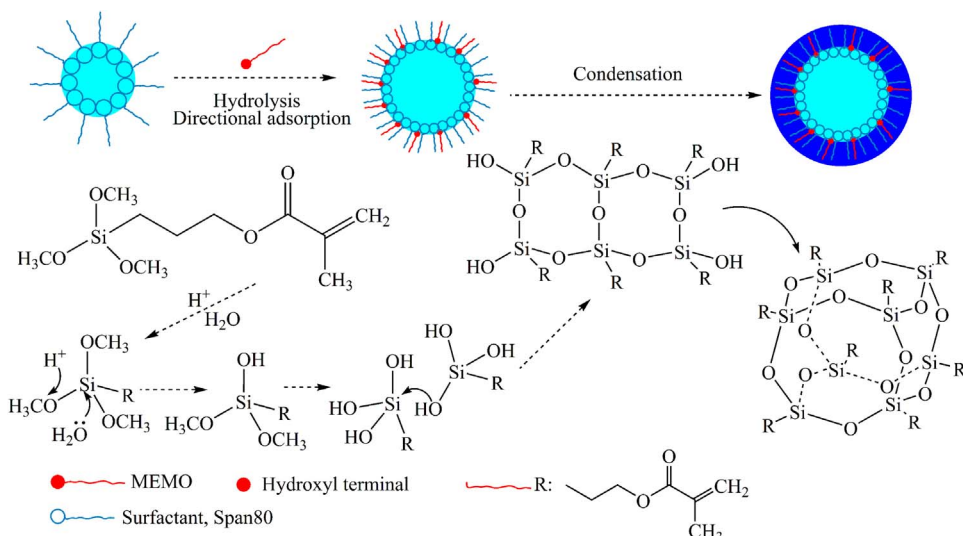
(approx.33.2 wt%), 0.30 g Span80 and 30 mL solvent were added in a beaker and dispersed under a magnetic stirrer at the room temperature for 15 min. Then, pH value of the mixture was adjusted to 2 using hydrochloric acid, and then certain amounts of MEMO, CMC or nano-α-Al_2O_3 were added. Afterward, the above turbid solution was dispersed vigorously by an ultra-turrax high speed homogenizer for 5 min and an ultrasonication cleaner for another 30 min at the same temperature to form W/O emulsion. This step is defined as hydrolysis and directional adsorption. In this step, the precursor of polysiloxane (MEMO) generated silanol through hydrolysis reaction and then adsorbed directionally on the W/O emulsion surface. (2) The emulsion was poured into a tailored low columned quartz container and irradiated by UV light for 2 h without stirring, which detailed in Ref [30]. In this process, the adsorbed silanol closed to each other by hydrogen-bond interaction and UV-assisted dehydration reaction occurred finally on the interface of oil-water. As a result, the capsules with shell-core structure, using ET as core and polysiloxane as shell, were formed due to the motion of hydrolysate restricted by intermolecular hydrogen bonding between ET and silanol. Finally, the white powder was collected, washed with ethyl alcohol several times, dried in a vacuum desiccator at 100 ˚C for 4 h and marked as ET/polysiloxane-condition. The sign of "condition" in the label stands for the fabricated condition of the blends. For example, ET/pSiO-toluene represents the composite synthesized using toluene as solvent. Analogously, ET/pSiO-1.5 C signifies the blends prepared with the addition of 1.5 wt% CMC (relative to ET).

2.3. Characterization

Thermal characteristics of ET and ET/polysiloxane composites were determined by DSC (NETZSCH DSC200F3, Netzsch Ltd. Germany) at the heating or cooling rate of 3 ˚C per min and temperature range from −20 ˚C to 140 ˚C in a purified nitrogen atmosphere. In the procedure of measurements, the as-prepared samples were heated higher than operating temperature and kept for 5 min firstly to erase the previous thermal history, afterword, it was cooled to −20 ˚C and heated again to determine the values of phase transition temperature and latent heat. In order to minimize the uncertainty and ensure reliability of the data, the instrument was calibrated with indium (99.999%). Due to the irreproducible crystallization temperatures of ET among parallel measurements [39], all samples were measured repeatedly and the average value of three repeated determinations was reported. The heat release ability, also called heat release percentage (HRP), is defined as the proportion of measured crystallization enthalpy (ΔH_c) in absorbed latent heat (ΔH_m) and calculated according to Eq. (1)

$$\text{Heat release percentage (\%)} = \frac{\Delta H_c}{\Delta H_m} \times 100\% \tag{1}$$

The chemical structure, including the changes in the compositional or functional group during fabrication and cycle test, was examined using a FT-IR spectroscope (Nicolet AVTAR 360, Thermo Electron Corp., U.S.A) with a KBr disk in the range of 4000–400 cm^{-1} at room temperature. The surface morphologies were characterized using a field-emission scanning electron microscope (JSM-6701, JEOL Ltd., Japan) in room temperature at an acceleration voltage of 20 kV. The specimens were prepared electrically conductive by sputter coating with a thin layer of gold in vacuum conditions to avoid charge accumulations. The microstructures were investigated by transmission electron microscopy (TEM, JEM-1200EX, JEOL Ltd., Japan) operating at an accelerating voltage of 100 kV. Before the investigation, all specimens were dispersed in ethanol by ultrasonicator (Kunshan, KQ3200DE, China). Thermal stability was detected using a thermogravimetric analyzer (TGA, NETZSCH STA-449F3, Netzsch Ltd. Germany) under an inert nitrogen atmosphere at a flow rate of 20 mL/min and a scanning rate of 5 ˚C/min in the range of 20 ˚C to 800 ˚C. To investigate the crystalline structure and stability of ET and ET/pSiO composites, powder X-ray diffraction patterns were recorded by X-ray diffractometer (XRD-6000, Daojin Ltd., Japan) using Cu K$_\alpha$ radiation (λ = 0.1542 nm) at a rate of 4˚/min in the range of 2˚ to 80˚. Thermal conductivity (κ) of ET and encapsulated ET was determined using a laser flash thermal conductivity instrument. Before measurement, the sample was pressed in to a cylindrical disk with thickness about 2 mm and diameter about 10 mm under the pressure of 10 MPa. Thermal reliability was also evaluated using DSC analyzer, FT-IR spectrophotometer and TGA using cycled products as specimens. The detail of accelerated thermal cycling experiment is described in our previous studies [30].

3. Results and discussion

3.1. Effect of solvent and temperature on thermal performance of ET/pSiO composite

Solvent and assembling temperature play vital roles in the hydrolysis of 3-methacryloxypropyltrimethoxysilane. In general, the molecular weight of polysiloxane increases with the increase of reaction temperature. However, dehydrating action will be occurred and the silicon hydroxyl groups (Si-OH) will transform into Si-O-Si groups if the temperature is higher than the boiling point of methanol (64.7 ˚C). Therefore, for the purpose of saving energy or increasing the reaction
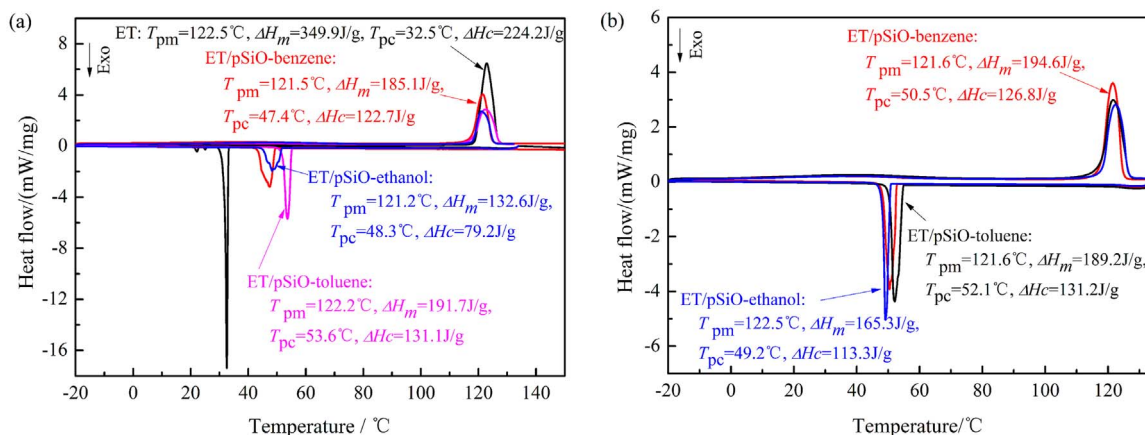
Fig. 2. DSC curves of ET and ET/pSiO prepared at 25 °C (a) and 60 °C (b) with different solvents.

speed, hydrolysis temperatures were restricted to 25 °C and 60 °C to investigate the influences of solvent and temperature on the thermal energy storage ability and thermal stability of the as-prepared composite. According to the published literature, erythritol is identified with two crystalline forms at least, a metastable polymorph and a stable crystalline [8,22,40]. The stable crystalline form is only obtained upon heating the frozen solid or leaving it for several hours at room temperature [9,25]. Therefore, all of samples for detection were stored for

two days parallelly before use. Fig. 2 shows the DSC curves of ET and ET/pSiO composite PCMs which synthesized in different solvent conditions. From Fig. 2, ET melt at 122.5 °C with the latent heat of 349.9 J g^{-1} and freeze at 32.5 °C with the enthalpy of 224.2 J g^{-1}, while the capsules melt around 122 °C and crystallize from 47.4 °C to 53.6 °C. The overlapping curves of melting indicate that the thermal energy storage ability of ET/pSiO comes from ET, and the increased crystallization temperature means the degree of supercooling of ET was
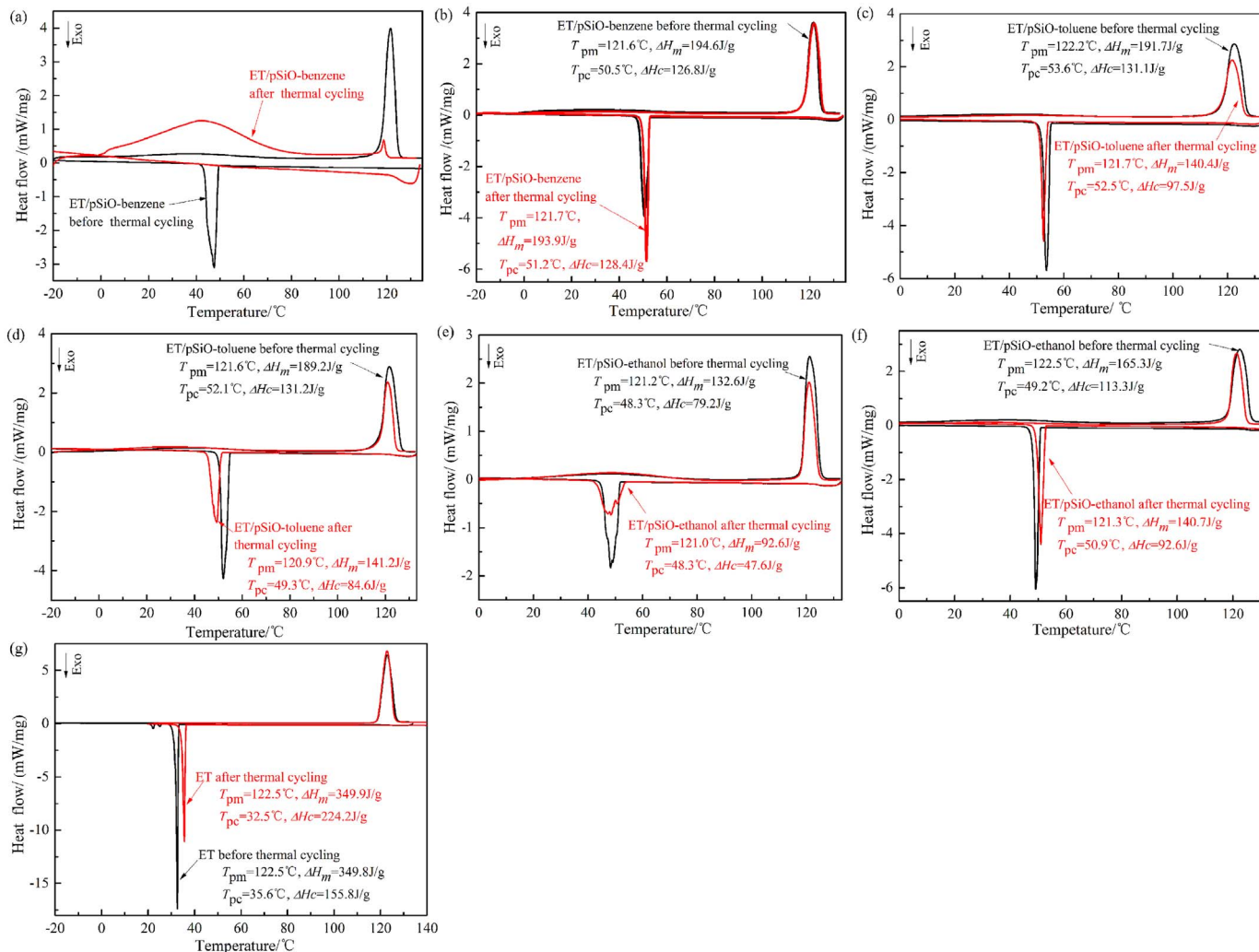

Fig. 3. DSC curves of ET/pSiO-benzene (a, b), ET/pSiO-toluene (c, d), ET/pSiO-ethanol (e, f) and ET (g) before and after thermal cycling fabricated at 25 °C (a, c, e) and 60 °C(b, d, f).

suppressed by encapsulation. Thanks for the large subcooling, 90 °C in present study consisted with the observation of A. Sari [11,12], the distinct relaxation of supercooling in ET/pSiO capsules strongly supported the idea that capsulation could decrease the supercooling degree of the PCMs [8,28–31]. On the other hand, the enthalpy of ET/pSiO fabricated at 25 °C using benzene, toluene and ethanol as solvent are found to be 185.1 J g^{-1}, 191.7 J g^{-1}, 132.6 J g^{-1} for melting and 122.7 J g^{-1}, 131.1 J g^{-1}, 79.2 J g^{-1} for crystallization, while it is 194.6 J g^{-1}, 189.2 J g^{-1}, 165.3 J g^{-1} and 126.8 J g^{-1}, 131.2 J g^{-1}, 113.3 J g^{-1} for ET/pSiO prepared at 60 °C, respectively. It is clearly can be seen that the capsules synthesized at 60 °C have better heat storage ability than those prepared at room temperature due to the complete hydrolysis of MEMO. However, the heat release ability (proportion of energy can be used in total stored heat) is 64% approximately for ET, meanwhile, it is about 65.2% for the composite. This result indicates that encapsulation is benefit for supercooling relaxation but has insignificant influence on the enhancement of heat release performance.

Fig. 3 demonstrates the effect of solvent and temperature on the stability of the assembled composite. As seen in Fig. 3, heat storage and release reliability of the capsules differed from the preparing conditions. The melting and crystallization latent heat of the cycled composite PCMs fabricated at 60 °C are all higher than that of the blends synthesized at 25 °C in each solvents, indicating that 60 °C is quite suitable for preparing ET/pSiO composites due to the fast reaction rate and complete coating. Although heat release performance is degenerated for some capsules, the DSC curves proved it again that capsulation is benefit for supercooling suppression. From another aspect, the heat release abilities of cycled products are all decreased except for the ET/pSiO-benzene prepared at 60 °C comparing with the fresh composite. The typical thermal parameters, including extrapolated onset temperature (T_{om} and T_{oc}), peak temperature (T_{pm} and T_{pc}), extrapolated end temperature (T_{em} and T_{ec}) and enthalpy ($\triangle H_m$ and $\triangle H_c$) for melting (m) and crystallization(c) of fresh and cycled ET and ET/pSiO-benzene synthesized at 60 °C, are shown in Table 1. From Fig. 3(g) and Table 1, it can be seen that the latent heat of pure ET decreases sharply, losing up to 56.6% of the initial value after 100 thermal cycling. This result indicates that the feasibility of using ET directly for thermal energy storage is hindered by poorly controlled heat release property, which is consistent with the result of S. Puupponen [39] and S. Y. Lee [41]. However, ET/pSiO-benzene before and after 100 thermal cycling has insignificant variation of phase transition temperature, crystallization and melting latent heat. Moreover, the heat release ability of suffered ET/pSiO-benzene is almost same with the original blends suggesting that the blends are more suitable for thermal energy storage than neat ET and encapsulation can improve the exothermicity of ET effectively.

3.2. Effect of core-shell mass ratio on the shape stability of ET/pSiO composite

As we all know, heat storage capacity is contradicted with the weight or thickness of shell in microencapsulated PCMs. Therefore, determining optimal core-shell mass ratio is necessary. To identify the maximum content of ET in composite without leakage, a series of composites with ET mass fraction from 40% to 80% were prepared at
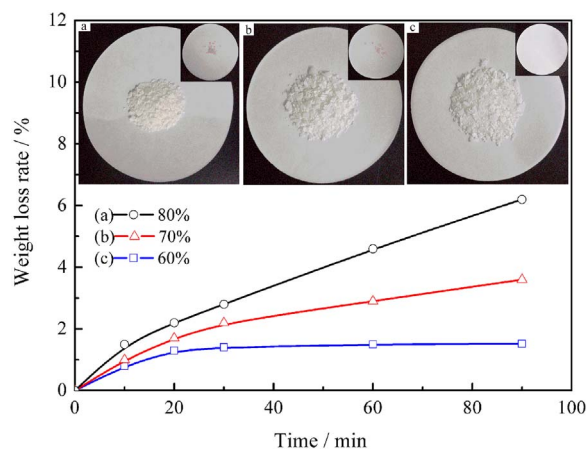

Fig. 4. Weight change curves and leakage photographs of ET/pSiO with different composition.

60 °C using benzene as solvent. In order to ensure the as-prepared samples are all form-stable and not leaky, all of pre-drying specimens fabricated in different recipes were placed on the filter papers and heated in an oven at 130°C for 10 min, 20 min, 30 min, 60 min and 90 min, respectively. The leakage was determined by gravimetric analysis and visual surface inspection. Only the samples which have no or insignificant mass changes were defined as form-stabilized MEPCMs and used for further investigation. The weight change curves and leakage photographs of some typical specimens are shown in Fig. 4. It can be seen from Fig. 4, the weight loss ratio increased with the extension of heating time in the first 30 min, and then tended to constant and the total weight changes was less than 1% of the composite with the core-shell mass ratio of 60%. On the contrary, the weight loss continued with the increase of time when mass ratio is higher than 60%. Therefore, the optimal ET mass fraction of 60% was used to fabricate ET/pSiO composite in subsequent studies.

3.3. Effect of additional agents on the thermal performance of ET/pSiO composite

Although supercooling degree and heat discharge performance of ET are reduced by 18.5 °C and improved by 21.7% compared with cycled ET (Table. 1) through microencapsulation, the subcooling is still large and thermal discharged performance is also poor. Therefore, the influences of annexing agent on subcooling of ET/pSiO which prepared under the existence of benzene at 60 °C were investigated and the related data originated from DSC measurement are presented in Table 2. The corresponding DSC curves and the effects of carboxymethylcellulose (CMC) amount on the supercooling are shown in Fig. 5. From Fig. 5(a), (b) and Table 2, the subcooling degree of encapsulated ET is suppressed significantly with small amount of CMC, and then enlarged slightly with increasing additive amount and afterwards maintained consistent. This result is coincided with the discovery of P. Hu [42] and M. Dannemand [43]. They selected CMC as the thickener for sodium acetate trihydrate (SAT) to prevent supercooling and the results showed that no supercooling phenomena occurred when

Table 1
Thermal physical parameters of original and cycled ET, ET/pSiO-benzene fabricated at 60 °C.

Samples	Solid–liquid phase transition				Liquid–solid phase transition				Degree of supercooling /°C	HRP (%)
	T_{om} (°C)	T_{pm} (°C)	T_{em} (°C)	$\triangle H_m$ (J/g)	T_{oc} (°C)	T_{pc} (°C)	T_{ec} (°C)	$\triangle H_c$ (J/g)		
ET	118.6	122.5	126.4	349.9	33.9	32.5	32.2	224.2	90.0	64.1
Cycled ET	118.6	122.5	126.5	349.8	36.4	35.6	32.5	155.8	86.9	44.5
ET/pSiO-benzene	114.8	121.6	125.9	194.6	53.3	50.5	46.9	126.8	71.1	65.2
Cycled ET/pSiO-benzene	114.8	121.6	126.0	193.9	53.3	51.2	48.9	128.4	70.4	66.2

Table 2
Thermographic data of ET/pSiO with different amounts of CMC and nano-alumina originated from DSC measurements.

Samples	Solid–liquid phase transition				Liquid–solid phase transition				Degree of supercooling /°C	HRP (%)
	T_{om} (°C)	T_{pm} (°C)	T_{em} (°C)	$\triangle H_m$ (J/g)	T_{oc} (°C)	T_{pc} (°C)	T_{ec} (°C)	$\triangle H_c$ (J/g)		
ET/pSiO-1.5C	114.2	120.8	125.5	212.0	112.1	107.1	103.2	207.6	13.7	97.9
ET/pSiO-3C	115.6	122.1	127.5	211.5	110.7	105.8	100.9	207.5	16.3	98.1
ET/pSiO-4.5C	112.0	120.8	126.5	206.6	109.2	103.7	97.1	204.8	17.1	99.2
ET/pSiO-6C	110.6	121.5	128.3	199.6	109.6	104.1	96.7	197.9	17.4	99.2
ET/pSiO-1.5A	115.9	120.9	124.6	154.2	107.2	101.4	98.4	140.0	19.5	90.8
ET/pSiO-3A	114.7	121.2	125.9	178.0	109.3	105.3	101.3	169.3	15.9	95.1
ET/pSiO-4.5A	116.2	121.6	125.9	204.4	107.5	99.5	97.1	190.9	22.1	93.4
ET/pSiO-6A	115.3	121.9	127.1	228.5	49.7	48.3	45.2	151.0	73.6	66.1

adding 5 wt% AlN nanoparticles and 4 wt% CMC [42] or introducing 5 wt% CMC and 5% graphite flakes to it [43]. Similar law also emerged into the relationship between additive amount and heat discharged performance. The ET/pSiO-1.5 C has minimum subcooling and relatively higher heat discharge ability which is measured as 13.7 °C and 97.9%, decreased by 76.3 °C and increased by 33.8% compared with neat ET. Moreover, from Fig. 5(c), the cycled ET/pSiO-1.5 C melt at 120.7 °C and freeze at 105.9°C with the latent heats of 210.6 J/g and 201.4 J/g, respectively. The subcooling degree and heat released percentage are measured as 14.8 °C and 95.4%.

Fig. 6 exhibits the effect of additive amount of nano-aluminium oxide (Nano-α-Al$_2$O$_3$) on the supercooling and HRP of encapsulated ET. The related data are also presented in Table 2. It can be seen from Fig. 6 and Table 2 that the supercooling degree of coated ET is relaxed firstly, and then bounce with the increase of α-Al$_2$O$_3$ amount when it is larger than 3.0 wt%, as well as the enhancement and degeneration of heat release ability. The suitable addition amount of α-Al$_2$O$_3$ is 3.0 wt%,

relative to the weight of pure ET. The ET/pSiO-3A has minimum supercooling and optimal heat release ability which are determined as 15.9 °C and 95.1%, respectively. From Fig. 6(c), the melting and freezing temperature and the corresponding phase change enthalpy of cycled ET/pSiO-3A are determined as 121.5 °C, 103.4 °C and 176.5 J/g, 158.9 J/g, respectively. The subcooling degree and HRP are 18.1 °C and 90%, increased by 2.2 °C and decreased by 5.1% compared with the fresh blends. Combining with the results of influence of CMC, it's tempting to conclude that there is a positive correlation between heat discharge performances and supercooling of ET. The appropriate decrease of supercooling is benefit for enhancement the heat discharge ability. Also, the reasonable changes and better reliability of ET/pSiO with additives compared with those of ET and encapsulated ET indicate that adding thickener or nano-particles is an effective method to relax supercooling and enhance heat discharged ability.

Although supercooling is one of the common phenomena in nature, it is still new to researchers and the factors influencing degree of
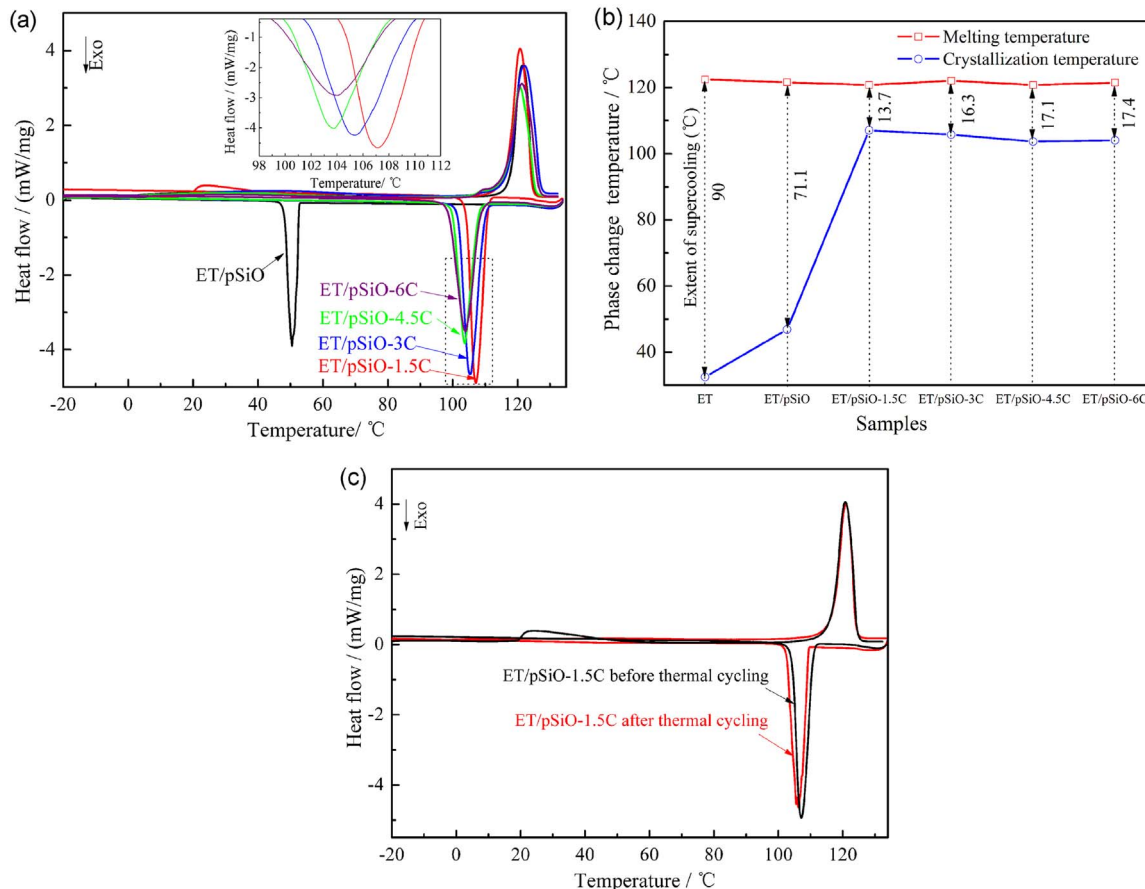

Fig. 5. DSC curves (a), comparison of supercooling degree (b) of ET/pSiO with different amount of CMC and stability of ET/pSiO-1.5 C before and after thermal cycling (c).
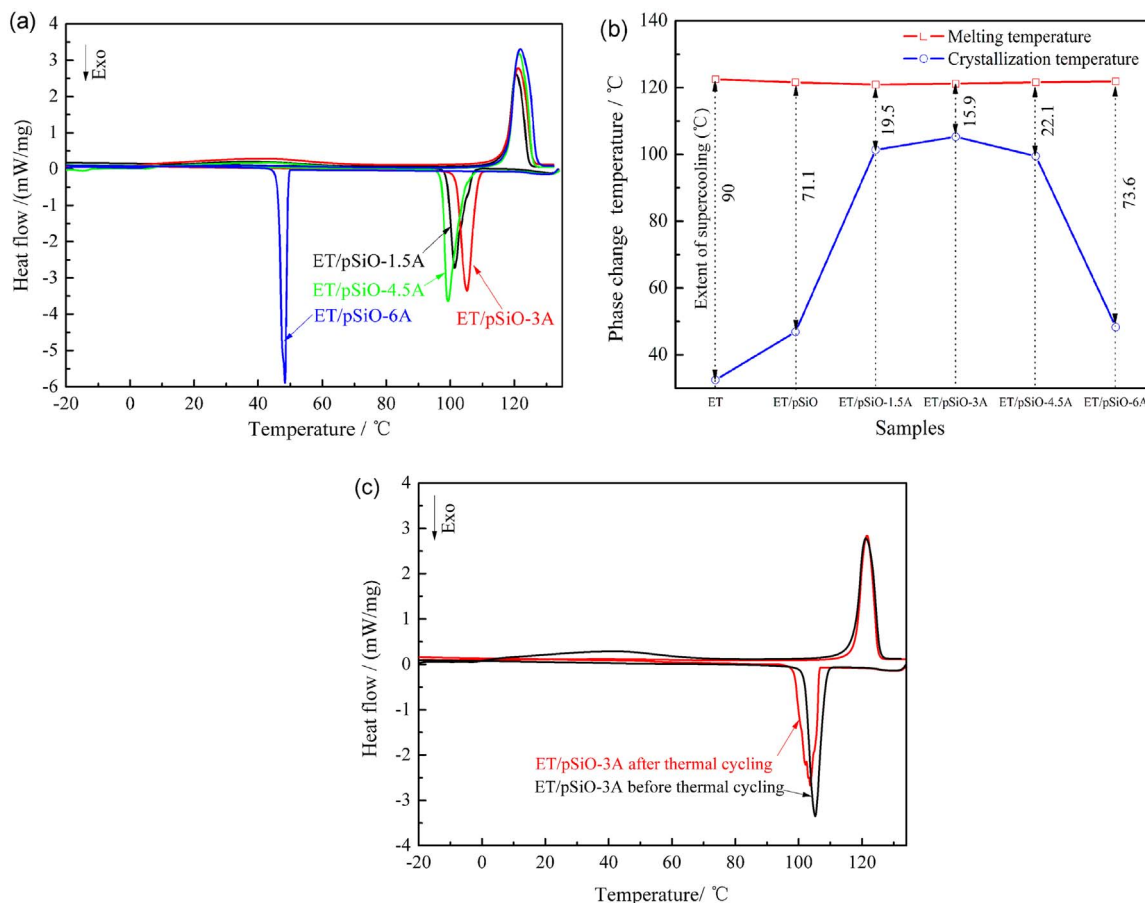
Fig. 6. DSC curves (a), comparison of supercooling degree (b) of ET/pSiO with different amount of nano-alumina and stability of ET/pSiO-3A before and after thermal cycling (c).

supercooling have not been clarified in literatures [44]. Therefore, the possible mechanism of supercooling degree inhibition using nucleating and thickening agents is discussed. Fig. 7 shows the DSC curves when ET was heated to different temperatures and supercooling curves of ET, encapsulated ET with different amount of CMC and α-Al$_2$O$_3$. It can be seen from Fig. 7(a) that ET release the absorbed heat and possess similar degree of supercooling, whether in a partially or fully melting state. This result suggests that the phase change behavior of ET is totally different from hydrous salt, such as SAT. In previous study, X. Jin [45] indicated that SAT was not able to release heat and could not absorb heat in the subsequent heating process if it was heated to fully melting state. However, SAT would quickly solidify and the supercooling could be significantly prevented without adding any nucleating agents if it melts partially and the temperature range are controlled properly. From the cooling curve of ET, Fig. 7(b), the temperature firstly takes a long time to drop to melting temperature and form nuclei implying liquid ET has low thermal diffusivity, and then, when nucleation begins, the temperature rises to anther temperature which lower than melting point due to the release of solidification latent heat indicating ET has poor crystallization kinetics [42]. From the Fig. 7(b) and (c), the cooling curves of encapsulated ET with thickener and nucleating agent, it easily can be seen that CMC and α-Al$_2$O$_3$ have significant influences on the onset time of nucleation and supercooling degree. For example, the nucleation starting time of ET/pSiO-1.5C is about 253 s, which is ahead of 202 s and is decreased by 44.5% than the time needed in ET (approx. 455 s). Moreover, it seems that the composite with shorten nucleation onset time also has suppressed subcooling degree. This finding confirms that the crystallization of ET is a "kinetic controlled" process and using CMC and α-Al$_2$O$_3$ can improve the crystallization rate. According to literature, the high crystallization rate of encapsulated ET with nucleating agent is caused by heterogeneous

nucleation of ET on the α-Al$_2$O$_3$ surface [46] and benefits from the increased interface surface area of shell material [19]. The rapid crystallization rate of coated ET with thicker may attribute to the restricted molecular motion area and increased regional undercooling because of the enhanced viscosity.

3.4. Morphology and chemical characteristics of ET/pSiO composite

Microcapsules can be made in an irregular shape or a regular shape, such as spherical, tubular, oval and etc. The morphologies of ET, polysiloxane, ET/pSiO-1.5C-3A prepared in the existence of benzene at 60 °C using 1.5 wt% CMC as thicker and 3 wt% α-Al$_2$O$_3$ as nucleating agent are illustrated in Fig. 8. As shown in Fig. 8, ET crystal has a polyhedral structure with smooth surface, while polysiloxane particle has an irregular shape with sharp edge. The morphology of ET/pSiO-1.5C-3A also has polyhedral shape with sharp edge, similar to the appearance of polysiloxane except a little fluffy surface. This finding indicates that the composite is fabricated by depositing polysiloxane on the surface of ET and copied the original morphological structure of ET. The obvious core-shell structure in Fig. 8(d) and the image with dark center and gray margin in Fig. 8(e) also confirmed this result. Therefore, the capsules are fabricated as our original plan.

Fig. 9 represents the FTIR spectra of ET, polysiloxane and ET/pSiO-1.5C-3A capsules. In the pure SA spectrum, the broad and strong absorption peak at 3250 cm^{-1} is corresponded to the vibration of O-H group. This characteristic adsorption indicates that the indistinctive intermolecular hydrogen bonds are formed since the stretching vibration of a free OH group in hydroxyl compounds is around 3630 cm^{-1} [9]. The peaks at 2968 cm^{-1} and 2908 cm^{-1} are attributed to the C-H asymmetric and symmetric stretching vibrations, respectively. The other typical characteristics, located at 1416 cm^{-1}, 1080 cm^{-1},
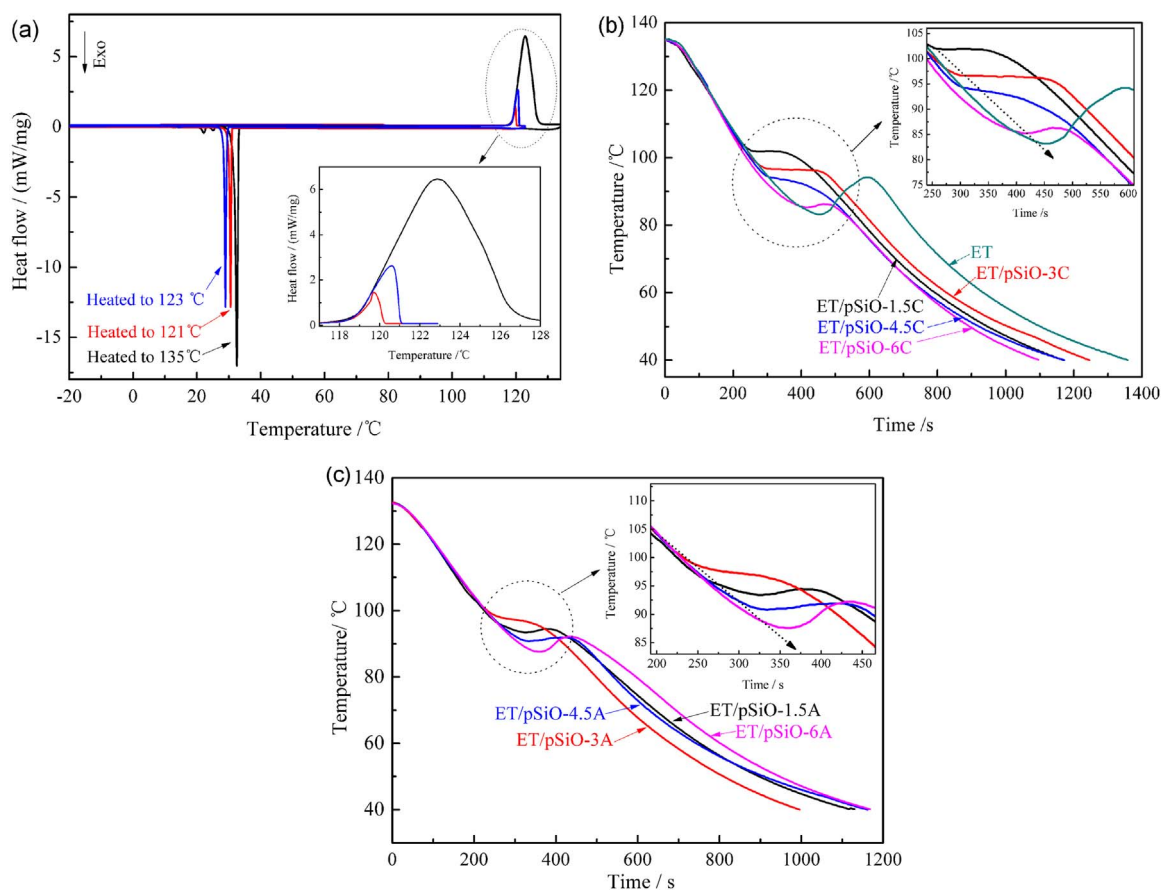
Fig. 7. DSC curves of ET heated to different temperatures (a), supercooling curve of ET and encapsulated ET with different amount of CMC (b) and α-Al₂O₃ (c).

1047 cm^{-1}, of carbohydrates were also observed [9,12,47]. In the typical FT-IR of polysiloxane, peaks observed at 3457 cm^{-1}, 2953 cm^{-1} and 2890 cm^{-1} belongs to the stretching vibration of O-H group, asymmetric and symmetric stretching vibration of aliphatic chain, respectively. The bands at 1728 cm^{-1} and 1636 cm^{-1} are assigned to the stretching vibration of carbonyl groups and carbon-carbon double bonds which are derived from the MEMO structure. The characteristic peak at 1107 cm^{-1} is caused by the stretching vibration of silicon-oxygen group. These results, especially the invisible adsorption peak of methoxyl, suggest that the shell material is the hydrolyzed and polymerized products of MEMO. Comparing the FT-IR spectra of neat ET, polysiloxane and ET/pSiO-1.5C-3A capsules, it is clear that the FT-IR spectrum of the capsules is composed by both peaks of ET and polysiloxane. No obvious new peaks were observed, which indicates that the chemical properties of erythritol would not be greatly changed by encapsulation and there is no chemical reaction occurred between core and shell in the fabricated process.

Fig. 10 displays the X-ray powder diffraction patterns of erythritol, polysiloxane and ET/pSiO-1.5C-3A capsules. The hydrolysate has the typical bread peak declaring it is amorphous [48]. As shown in diffractogram of ET, ET has numerous narrow peaks with the most intense ones located at $2\theta = 14.5°$, $19.5°$, $20.3°$, $24.5°$ and $29.8°$, which is in consistent with the report of A. J. L. Jesus [9] and S. Tanimura [48]. The peak at $2\theta = 21°$ ascribed to the metastable phase has not been observed due to leaving the samples for 2 days at room temperature. The XRD pattern of ET/pSiO-1.5C-3A has similar characteristic diffraction peaks associated to the crystalline structure of erythritol except for the reduced intensity. This result indicates that ET was well coated and the encapsulated ET has the original crystalline arrangement regardless of whether it is embedded and doped.

3.5. Thermal properties, reliability and stability of ET/pSiO composite

As a potential candidate, it should be shown no or less change in its thermal properties and chemical structure after long term using period. Fig. 11 shows the thermal conductivity, normalized latent heat and supercooling degree, heat storage/release curves of ET/pSiO-1.5C-3A before and after 200th repeated thermal cycling. From Fig. 11(a), the thermal conductivity of the pristine ET is 0.65 W/m K at 25 °C. However, the thermal conductivities of ET/pSiO and ET/pSiO-1.5C-3A are measured as 0.72 W/m K and 0.84 W/m K, respectively, increased by 10.8% and 29.2% comparing to neat ET due to encapsulation and additive addition. The enhanced thermal conductivity means that the composite has better heat charging and discharging performance. The composite also has high stability during the accelerated thermal cycles with negligible change in the values of melting/solidification latent heat and supercooling (Fig. 11(b)) although ET has significant expansion coefficient of 14% [19]. The DSC curves of ET/pSiO-1.5C-3A before and after 200 cycles, inserted in Fig. 11(b), show that the phase change temperatures and latent heats of melting and freezing are 121.2 °C, 106.4 °C and 213.3 J/g, 206.9 J/g for original composite, as well as 121.3 °C, 106.2 °C and 208.4 J/g, 201.6 J/g for cycled blends, respectively. The measured subcooling degree and heat retrieval performance are 14.8 °C and 96.9% for fresh material, while they are 15.1 °C and 96.7% for cycled blends. These values correspond to a 75 °C suppression for subcooling degree and a 52.5% increase for heat release ability compared with those of neat ET. From Fig. 11(c), the representative heating and cooling curves of uncycled and cycled ET/pSiO-1.5C-3A, it also can be obviously observed that the heating and cooling temperature curves of the blends before and after thermal cycling have less change. The constant supercooling degree, unchanging heat release ability and matched heat storage/retrieval performance all
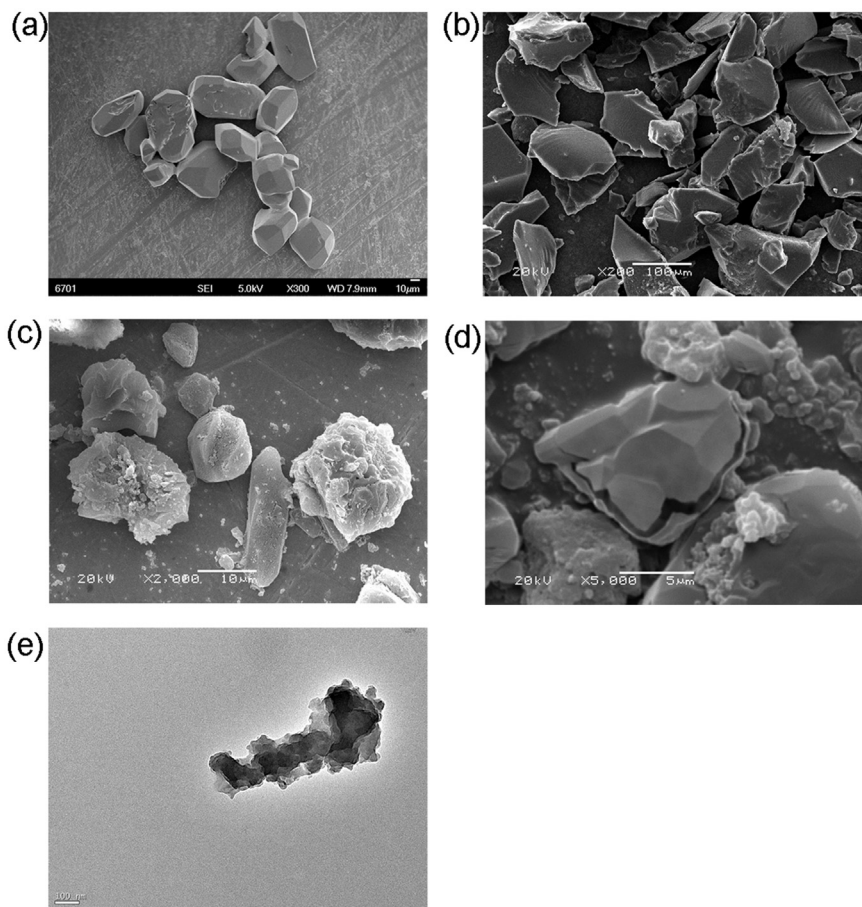
Fig. 8. SEM micrographs of ET (a), polysiloxane (b), ET/pSiO-1.5C-3A (c, d) and TEM image of ET/pSiO-1.5C-3A (e).
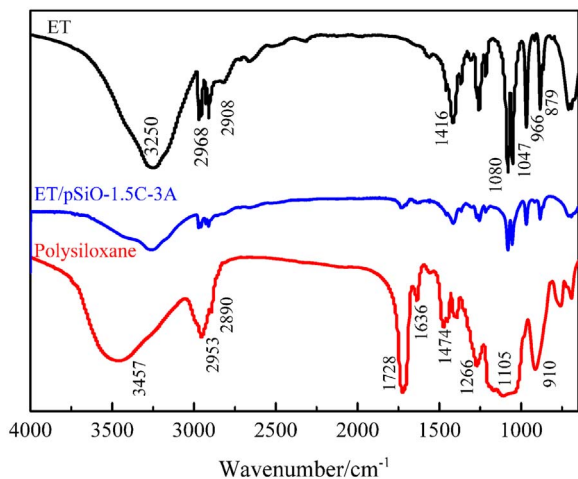

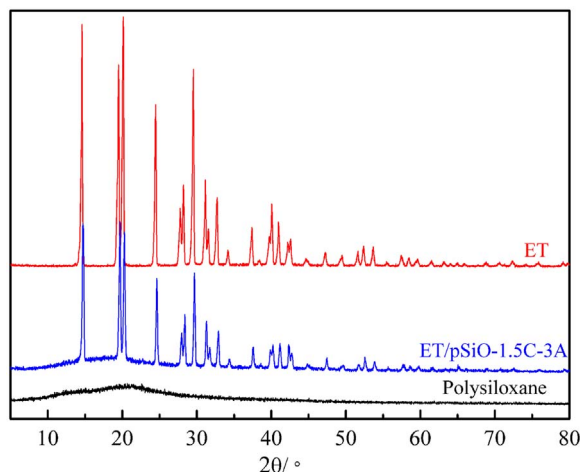**Fig. 9.** FTIR spectra of ET, polysiloxane and ET/pSiO-1.5C-3A capsules.

Fig. 10. X-ray powder diffraction patterns of erythritol, polysiloxane and ET/pSiO-1.5C-3A capsules.

indicate that ET/pSiO-1.5C-3A has good reliability for recycled utilization.

The changes in the functional group and crystal form of capsulated ET before and after 200 heating-cooling cycles were investigated by FT-IR and XRD technique and the results are shown in Fig. 12. As seen from the FTIR spectra, Fig. 12(a), the shape and frequency of characteristic absorption peaks are highly close before and after thermal cycling. Also, negligible changes about the position and intensity of the diffraction peaks are observed in the XRD patterns, Fig. 12(b). These evidences of good chemical stability indicate that ET/pSiO-1.5C-3A can be reused without degradation.

Thermal durability of ET and ET/pSiO-1.5C-3A were determined by

thermogravimetry and the TGA profile is shown in Fig. 13. It can be clearly observed that ET is stable up to 200 °C and then decomposes sharply, which is similar to the observation of M. Karthik [25]. Despite ET and cycled ET has different latent heat, Fig. 3(g), the TG curves overlapped completely. This result declares that ET has good thermal durability when it is used under the decomposition temperature. The ET/pSiO-1.5C-3A shows a three-stage mass loss process. The negligible weight changes before 150 °C and the third mass loss stage larger than 350 °C are corresponding to the elimination of some volatile species and the degradation of polysiloxane, respectively. The second step with 59.2 wt% losses at temperature range of 228 °C to 335 °C is attributed
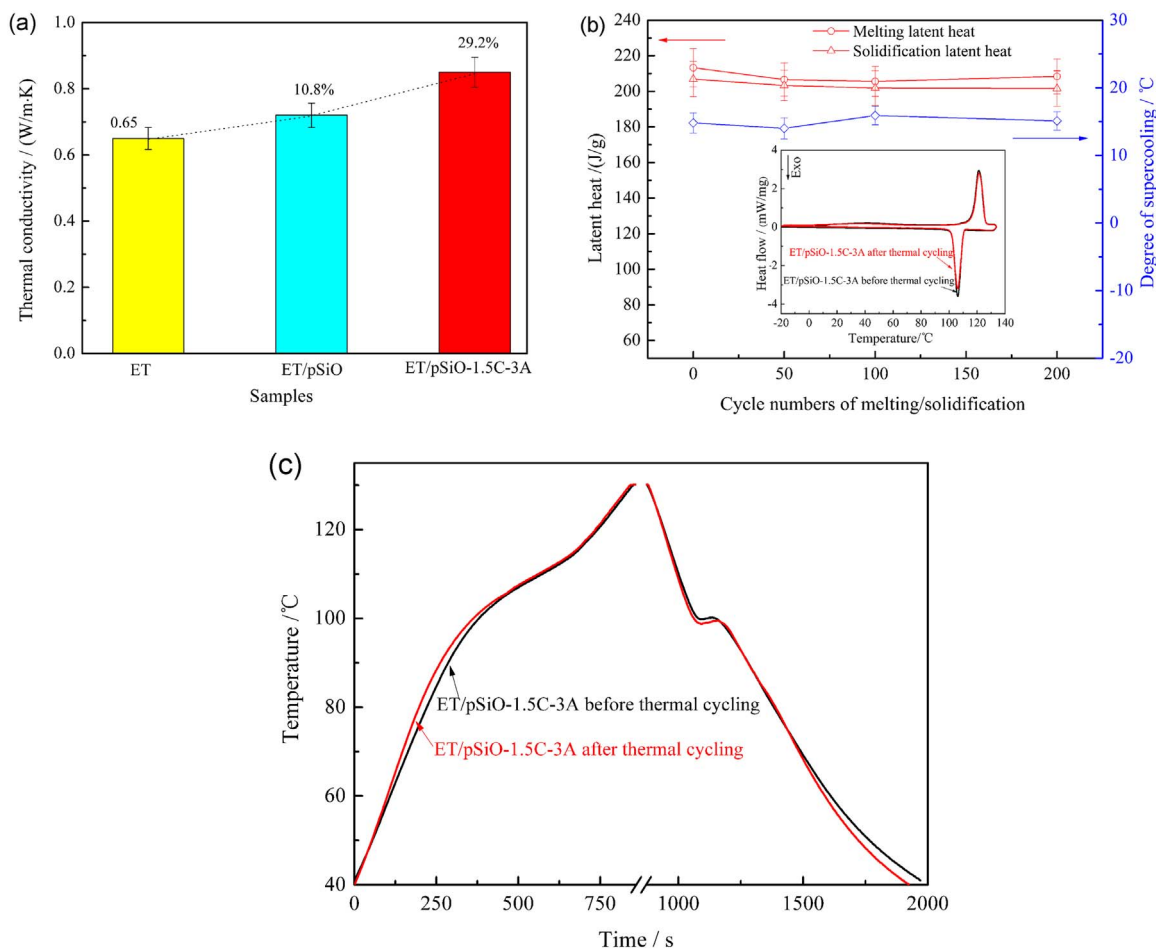
Fig. 11. Graph of thermal conductivity (a), normalized latent heat and supercooling degree (b) and curves of heat storage/release for ET/pSiO-1.5C-3A before and after 200th repeated thermal cycling (c).

to the decomposition of ET. Therefore, it is reasonable to conclude that ET content in the composite is 59.2 wt%, which is close to the mass fraction in the preparation recipe and the value calculated by melting enthalpy indicates that all of ET in the fabricated solution are well coated. When take the TG curves of capsulated ET before and after cycles into comparison, it is obvious that the variations of weight loss before and after thermal cycling are nearly overlapped in all investigated range. This means that the composite PCM has good thermal stability and no degradation occurred when it serves at the working temperature range.

4. Conclusion

In summary, polysiloxane capsules containing erythritol as a stable PCM were obtained by ultraviolet assisted hydrolysis method using carboxymethylcellulose as nucleating agent and nano-alumina as thicker. The structure and thermo-physical properties of the composite, especially the effects of encapsulation and additives on the supercooling relaxation and exothermicity improvement, were studied. From the results, it was found that the synthetic conditions have positive influence on the thermal storage ability and stability of the composite. The
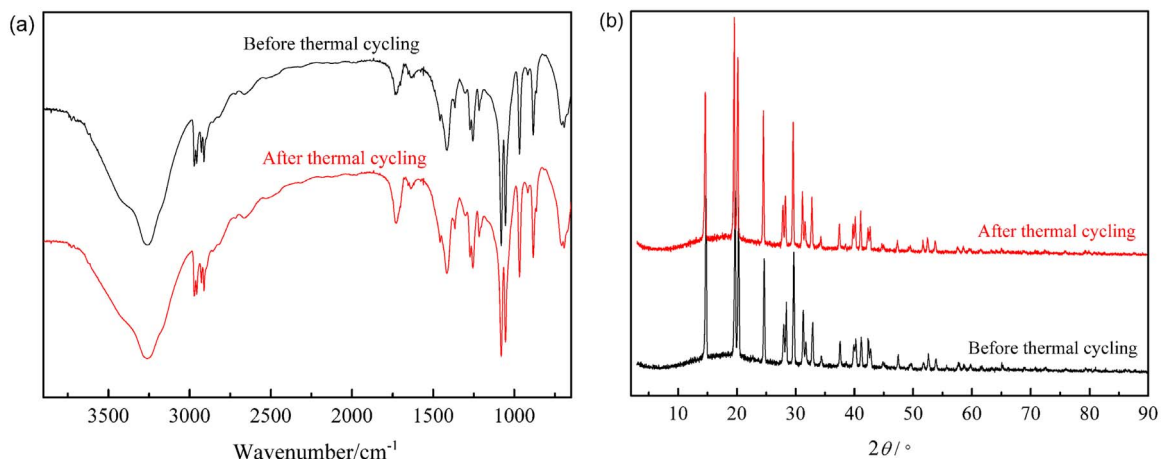

Fig. 12. FT-IR spectra (a) and XRD patterns (b) of ET/pSiO-1.5C-3A before and after 200 heating-cooling cycles.
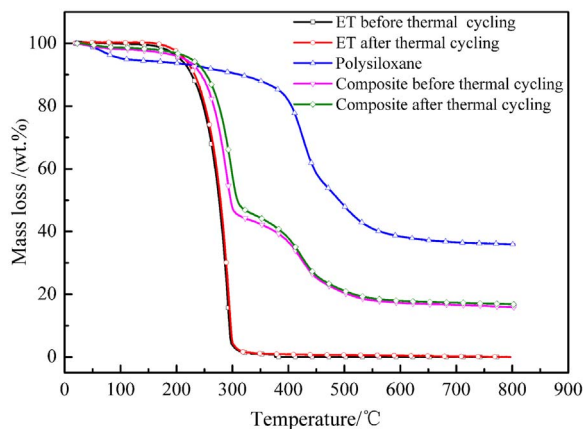
Fig. 13. TG curves of polysiloxane and ET, ET/pSiO-1.5C-3A before and thermal cycling.

optimum condition of preparation was hydrolyzed at 60 °C using benzene as solvent. Under this condition, the degree of supercooling was decreased by 18.9 °C through encapsulation, while it reduced by 75.2 °C along with the increase of heat release performance from 44.5% to 96.7% by encapsulation and adding impurity. The capsuled ET containing nucleating and thickening agents has maximal mass percentage of 59.2% and obvious core-shell structure due to polysiloxane deposited on the surface and further copied the original morphological structure of ET crystal. The results of FT-IR and XRD clearly indicated that the composite has good compatibility between erythritol and polysiloxane, and capsulation and doping agents have no influences on the crystal structure. The thermal conductivity of the blends is 0.84 W/ m K at 25 °C, increased by 29.2% than pristine ET. Moreover, the composite showed negligible variations in thermal behavior, thermal durability and chemical structure. The above mentioned experimental results, especially the suppressed supercooling, enhanced heat release efficiency and increased thermal conductivity, demonstrated that the composite PCM can be considered as a potential material for thermal energy storage applications.

Acknowledgments

References

[1] Y.E. Milián, A. Gutiérrez, M. Grágeda, S. Ushak, A review on encapsulation techniques for inorganic phase change materials and the influence on their thermophysical properties, Renew. Sustain. Energy Rev. 73 (2017) 983–999.

[2] X. Huang, G. Alva, L. Liu, G. Fang, Preparation, characterization and thermal properties of fatty acid eutectics/bentonite/expanded graphite composites as novel form–stable thermal energy storage materials, Sol. Energy Mater. Sol. Cells 166 (2017) 157–166.

[3] Y. Wang, Y. Zhang, W. Yang, H. Ji, Selection of low temperature phase change materials for thermal energy storage based on the VIKOR method, Energy Technol. 3 (2015) 84–89.

[4] C. Alkan, A. Sari, A. Karaipekli, O. Uzun, Preparation, characterization, and thermal properties of microencapsulated phase change material for thermal energy storage, Sol. Energy Mater. Sol. Cells 93 (2009) 143–147.

[5] F. Kuznik, D. David, K. Johannes, J.J. Roux, A review on phase change materials integrated in building walls, Renew. Sustain. Energy Rev. 15 (2011) 379–391.

[6] V.V. Tyagi, S.C. Kaushik, S.K. Tyagi, T. Akiyama, Development of phase change materials based microencapsulated technology for buildings: a review, Renew. Sustain. Energy Rev. 15 (2011) 1373–1391.

[7] A. Kaizawa, N. Maruoka, A. Kawai, H. Kamano, T. Jozuka, T. Senda, T. Akiyama, Thermophysical and heat transfer properties of phase change material candidate for waste heat transportation system, Heat Mass Transf. 44 (2008) 763–769.

[8] S.N. Gunasekara, R. Pan, J.N. Chiu, V. Martin, Polyols as phase change materials for surplus thermal energy storage, Appl. Energy 162 (2016) 1439–1452.

[9] A.J.L. Jesus, S.C.C. Nunes, M.R. Silva, A.M. Beja, J.S. Redinha, Erythritol: crystal growth from the melt, Int. J. Pharm. 388 (2010) 129–135.

[10] H. Hidaka, M. Yamazaki, M. Yabe, H. Kakiuchi, E.P. Ona, Y. Kojima, H. Matsuda, New PCMS prepared from erythritol-polyalcohols mixtures for latent heat storage between 80 and 100 °C, J. Chem. Eng. Jpn. 37 (2004) 1155–1162.

[11] A. Sari, R. Eroğlu, A. Biçer, A. Karaipekli, Synthesis and thermal energy storage properties of erythritol tetrastearate and erythritol tetrapalmitate, Chem. Eng. Technol. 34 (2011) 87–92.

[12] A. Sari, A. Karaipekli, R. Eroğlu, A. Biçer, Erythritol tetra myristate and erythritol tetra laurate as novel phase change materials for low temperature thermal energy storage, Energy Source Part A 35 (2013) 1285–1295.

[13] T. Oya, T. Nomura, M. Tsubota, N. Okinaka, T. Akiyama, Thermal conductivity enhancement of erythritol as PCM by using graphite and nickel particles, Appl. Therm. Eng. 61 (2013) 825–828.

[14] T. Oya, T. Nomura, N. Okinaka, T. Akiyama, Phase change composite based on porous nickel and erythritol, Appl. Therm. Eng. 40 (2012) 373–377.

[15] E.P. Ona, X. Zhang, K. Kyaw, F. Watanabe, H. Matsuda, H. Kakiuchi, M. Yabe, S. Chihara, Relaxation of supercooling of erythritol for latent heat storage, J. Chem. Eng. Jpn. 34 (2001) 376–382.

[16] K. Nakano, Y. Masuda, H. Daiguji, Crystallization and melting behavior of erythritol in and around two-dimensional hexagonal mesoporous silica, J. Phys. Chem. C 119 (2015) 4769–4777.

[17] M.A. Kibria, M.R. Anisur, M.H. Mahfuz, R. Saidur, I.H.S.C. Metselaar, A review on thermophysical properties of nanoparticle dispersed phase change materials, Energy Convers. Manag. 95 (2015) 69–89.

[18] R. Al-Shannaq, J. Kurdi, S. Al-Muhtaseb, M. Dickinson, M. Farid, Supercooling elimination of phase change materials (PCMs) microcapsules, Energy 87 (2015) 654–662.

[19] I. Kholmanov, J. Kim, E. Ou, R.S. Ruoff, L. Shi, Continuous carbon nanotube ultrathin graphite hybrid foams for increased thermal conductivity and suppressed subcooling in composite phase change materials, ACS Nano 9 (2015) 11699–11707.

[20] Y. Liu, X. Li, P. Hu, G. Hu, Study on the supercooling degree and nucleation behavior of water-based graphene oxide nanofluids PCM, Int. J. Refrig. 50 (2015) 80–86.

[21] E.P. Ona, S. Ozawa, Y. Kojima, H. Matsuda, H. Hidaka, H. Kakiuchi, M. Sato, Effect of ultrasonic irradiation parameters on the supercooling relaxation behavior of PCM, J. Chem. Eng. Jpn. 36 (2003) 799–805.

[22] E.P. Ona, X. Zhang, S. Ozawa, H. Matsuda, H. Kakiuchi, M. Yabe, M. Yamazaki, M. Sato, Influence of ultrasonic irradiation on the solidification behavior of erythritol as a PCM, J. Chem. Eng. Jpn. 35 (2002) 290–298.

[23] T. Adachi, D. Daudah, G. Tanaka, Effects of supercooling degree and specimen size on supercooling duration of erythritol, ISIJ Int. 54 (2014) 2790–2795.

[24] X. Zhang, X. Chen, Z. Han, W. Xu, Study on phase change interface for erythritol with nano-copper in spherical container during heat transport, Int. J. Heat Mass Transf. 92 (2016) 490–496.

[25] M. Karthik, A. Faik, P. Blanco-Rodriguez, J. Rodríguez-Aseguinolaza, B. D'Aguanno, Preparation of erythritol–graphite foam phase change composite with enhanced thermal conductivity for thermal energy storage applications, Carbon 94 (2015) 266–276.

[26] Y. Liu, Y. Liu, P. Hu, X. Li, R. Gao, Q. Peng, L. Wei, The effects of graphene oxide nanosheets and ultrasonic oscillation on the supercooling and nucleation behavior of nanofluids PCMs, Microfluid. Nanofluid. 18 (2015) 81–89.

[27] L.L. Wei, K. Ohsasa, Supercooling and solidification behavior of phase change material, ISIJ Int. 50 (2010) 1265–1269.

[28] A. Sari, C. Alkan, A. Karaipekli, O. Uzun, Microencapsulated n-octacosane as phase change material for thermal energy storage, Sol. Energy 83 (2009) 1757–1763.

[29] G. Fang, H. Li, F. Yang, X. Liu, S. Wu, Preparation and characterization of nano-encapsulated n-tetradecane as phase change material for thermal energy storage, Chem. Eng. J. 153 (2009) 217–221.

[30] Y. Wang, Y. Zhang, T. Xia, W. Zhao, W. Yang, Effects of fabricated technology on particle size distribution and thermal properties of stearic–eicosanoic acid/polymethylmethacrylate nanocapsules, Sol. Energy Mater. Sol. Cells 120 (2014) 481–490.

[31] X. Tang, W. Li, H. Shi, X. Wang, J. Wang, X. Zhang, Fabrication, characterization, and supercooling suppression of nanoencapsulated n-octadecane with methyl methacrylate–octadecyl methacrylate copolymer shell, Colloid Polym. Sci. 291 (2013) 1705–1712.

[32] M. You, X. Wang, X. Zhang, L. Zhang, J. Wang, Microencapsulated n-Octadecane with styrene-divinybenzene co-polymer shells, J. Polym. Res. 18 (2011) 49–58.

[33] P. Chaiyasat, S. Noppalit, M. Okubo, A. Chaiyasat, Do encapsulated heat storage materials really retain their original thermal properties? Phys. Chem. Chem. Phys. 17 (2015) 1053–1059.

[34] Q. Wu, D. Zhao, X. Jiao, Y. Zhang, K.J. Shea, X. Lu, G. Qiu, Preparation, properties, and supercooling prevention of phase change material n-octadecane microcapsules with peppermint fragrance scent, Ind. Eng. Chem. Res. 54 (2015) 8130–8136.

[35] H. Wang, J.P. Wang, X. Wang, W. Li, X. Zhang, Preparation and properties of microencapsulated phase change materials containing two-phase core materials, Ind. Eng. Chem. Res. 52 (2013) 14706–14712.

[36] J.L. Alvarado, C. Marsh, C. Sohn, M. Vilceus, V. Hock, G. Phetteplace, T. Newell, Characterization of supercooling suppression of microencapsulated phase change material by using DSC, J. Therm. Anal. Calorim. 86 (2006) 505–509.

[37] J. Huang, T. Wang, P. Zhu, J. Xiao, Preparation, characterization, and thermal properties of the microencapsulation of a hydrated salt as phase change energy storage materials, Thermochim. Acta 557 (2013) 1–6.

[38] T. Nomura, N. Okinaka, T. Akiyama, Impregnation of porous material with phase change material for thermal energy storage, Mater. Chem. Phys. 115 (2009) 846–850.

[39] S. Puupponen, V. Mikkola, T. Ala-Nissila, A. Seppälä, Novel microstructured polyol-

polystyrene composites for seasonal heat storage, Appl. Energy 172 (2016) 96–106.

[40] G. Diarce, I. Gandarias, Á. Campos-Celador, A. García-Romero, U.J. Griesser, Eutectic mixtures of sugar alcohols for thermal energy storage in the 50–90 °C temperature range, Sol. Energy Mater. Sol. Cells 134 (2015) 215–226.

[41] S.Y. Lee, H.K. Shin, M. Park, K.Y. Rhee, S.J. Park, Thermal characterization of erythritol/expanded graphite composites for high thermal storage capacity, Carbon 68 (2014) 67–72.

[42] P. Hu, D.J. Lu, X.Y. Fan, X. Zhou, Z.S. Chen, Phase change performance of sodium acetate trihydrate with AlN nanoparticles and CMC, Sol. Energy Mater. Sol. Cells 95 (2011) 2645–2649.

[43] M. Dannemand, J.B. Johansen, S. Furbo, Solidification behavior and thermal conductivity of bulk sodium acetate trihydrate composites with thickening agents and graphite, Sol. Energy Mater. Sol. Cells 145 (2016) 287–295.

[44] A. Safari, R. Saidur, F.A. Sulaiman, Y. Xu, J. Dong, A review on supercooling of

phase change materials in thermal energy storage systems, Renew. Sustain. Energy Rev. 70 (2017) 905–919.

[45] X. Jin, M.A. Medina, X. Zhang, S. Zhang, Phase-change characteristic analysis of partially melted sodium acetate trihydrate using DSC, Int. J. Thermophys. 35 (2014) 45–52.

[46] Y. Liu, Y. Yang, Use of nano-α-Al_2O_3 to improve binary eutectic hydrated salt as phase change material, Sol. Energy Mater. Sol. Cells 160 (2017) 18–25.

[47] Z. Luo, Q. Zhang, G. Wu, Preparation and enhanced heat capacity of nano-titania doped erythritol as phase change material, Int. J. Heat Mass Transf. 80 (2015) 653–659.

[48] S. Tanimura, K. Tahara, H. Takeuchi, Spray-dried composite particles of erythritol and porous silica for orally disintegrating tablets prepared by direct tableting, Powder Technol. 286 (2015) 444–450.